REPORT DOCUMENTATION PAGE

Form Approved
OMB No. 0704-0188

PLEASE DO NOT RETURN YOUR FORM TO THE ABOVE ORGANIZATION.

1. REPORT DATE *(DD-MM-YYYY)*	2. REPORT TYPE	3. DATES COVERED *(From - To)*
19-01-2011	Final	15 March 2008- 30 November, 2010

4. TITLE AND SUBTITLE
MODELING OF THE ORIGIN AND ENERGIZATION OF THE INNER RADIATION BELT ELECTRONS AND PHENOMENA THAT MEDIATES IT

5a. CONTRACT NUMBER
FA9550-08-1-0140

5b. GRANT NUMBER

5c. PROGRAM ELEMENT NUMBER

6. AUTHOR(S)
Yuri Shprits

5d. PROJECT NUMBER

5e. TASK NUMBER

5f. WORK UNIT NUMBER

7. PERFORMING ORGANIZATION NAME(S) AND ADDRESS(ES)
DAOS, UCLA
405 Hilgard Ave / 7127 Math Sciences Bldg, Los Angeles, California

8. PERFORMING ORGANIZATION REPORT NUMBER

9. SPONSORING/MONITORING AGENCY NAME(S) AND ADDRESS(ES)
AFOSR
875 N. RANDOLPH ST.
SUITE 325
ARLINGTON, VA 22203

10. SPONSOR/MONITOR'S ACRONYM(S)
AFOSR

11. SPONSOR/MONITOR'S REPORT NUMBER(S)
AFRL-OSR-VA-TR-2012-0641

12. DISTRIBUTION/AVAILABILITY STATEMENT
Distribution A

13. SUPPLEMENTARY NOTES

14. ABSTRACT

We have computed scattering rates due to various plasma waves . The computed diffusion coefficients were incorporated into our 3D Versatile Electron Radiation Belts (VERB) diffusion code [Subbotin and Shprits, 2009; Shprits et al,. 2009]. We have also showed that another scattering mechanism (bounce resonance scattering) driven by magnetosonic waves plays a very important role for scattering radiation belt electrons [Shprits, 2009]. Our VERB code successfully reproduced the behavior of the radiation belts during the Halloween solar storms in 2003. We have also showed that during extremely strong storms, which have occurred in the past and may occur in the future, relativistic electrons will populate the inner belt (below 1.5 RE) , where enhanced relativistic electron fluxes may persist for several years [Shprits et al, 2010].

15. SUBJECT TERMS
Radiation Belts, Radiation hazard, Near-Earth radiation environment

16. SECURITY CLASSIFICATION OF:			17. LIMITATION OF ABSTRACT	18. NUMBER OF PAGES	19a. NAME OF RESPONSIBLE PERSON
a. REPORT	b. ABSTRACT	c. THIS PAGE			19b. TELEPHONE NUMBER *(Include area code)*

INSTRUCTIONS FOR COMPLETING SF 298

1. REPORT DATE. Full publication date, including day, month, if available. Must cite at least the year and be Year 2000 compliant, e.g. 30-06-1998; xx-06-1998; xx-xx-1998.

2. REPORT TYPE. State the type of report, such as final, technical, interim, memorandum, master's thesis, progress, quarterly, research, special, group study, etc.

3. DATES COVERED. Indicate the time during which the work was performed and the report was written, e.g., Jun 1997 - Jun 1998; 1-10 Jun 1996; May - Nov 1998; Nov 1998.

4. TITLE. Enter title and subtitle with volume number and part number, if applicable. On classified documents, enter the title classification in parentheses.

5a. CONTRACT NUMBER. Enter all contract numbers as they appear in the report, e.g. F33615-86-C-5169.

5b. GRANT NUMBER. Enter all grant numbers as they appear in the report, e.g. AFOSR-82-1234.

5c. PROGRAM ELEMENT NUMBER. Enter all program element numbers as they appear in the report, e.g. 61101A.

5d. PROJECT NUMBER. Enter all project numbers as they appear in the report, e.g. 1F665702D1257; ILIR.

5e. TASK NUMBER. Enter all task numbers as they appear in the report, e.g. 05; RF0330201; T4112.

5f. WORK UNIT NUMBER. Enter all work unit numbers as they appear in the report, e.g. 001; AFAPL30480105.

6. AUTHOR(S). Enter name(s) of person(s) responsible for writing the report, performing the research, or credited with the content of the report. The form of entry is the last name, first name, middle initial, and additional qualifiers separated by commas, e.g. Smith, Richard, J, Jr.

7. PERFORMING ORGANIZATION NAME(S) AND ADDRESS(ES). Self-explanatory.

8. PERFORMING ORGANIZATION REPORT NUMBER. Enter all unique alphanumeric report numbers assigned by the performing organization, e.g. BRL-1234; AFWL-TR-85-4017-Vol-21-PT-2.

9. SPONSORING/MONITORING AGENCY NAME(S) AND ADDRESS(ES). Enter the name and address of the organization(s) financially responsible for and monitoring the work.

10. SPONSOR/MONITOR'S ACRONYM(S). Enter, if available, e.g. BRL, ARDEC, NADC.

11. SPONSOR/MONITOR'S REPORT NUMBER(S). Enter report number as assigned by the sponsoring/ monitoring agency, if available, e.g. BRL-TR-829; -215.

12. DISTRIBUTION/AVAILABILITY STATEMENT. Use agency-mandated availability statements to indicate the public availability or distribution limitations of the report. If additional limitations/ restrictions or special markings are indicated, follow agency authorization procedures, e.g. RD/FRD, PROPIN, ITAR, etc. Include copyright information.

13. SUPPLEMENTARY NOTES. Enter information not included elsewhere such as: prepared in cooperation with; translation of; report supersedes; old edition number, etc.

14. ABSTRACT. A brief (approximately 200 words) factual summary of the most significant information.

15. SUBJECT TERMS. Key words or phrases identifying major concepts in the report.

16. SECURITY CLASSIFICATION. Enter security classification in accordance with security classification regulations, e.g. U, C, S, etc. If this form contains classified information, stamp classification level on the top and bottom of this page.

17. LIMITATION OF ABSTRACT. This block must be completed to assign a distribution limitation to the abstract. Enter UU (Unclassified Unlimited) or SAR (Same as Report). An entry in this block is necessary if the abstract is to be limited.

FINAL PROGRESS SUMMARY

To: technicalreports@afosr.af.mil

Subject: Final Progress Report

Contract/Grant Title: (YIP-09) MODELING OF THE ORIGIN AND ENERGIZATION OF THE INNER RADIATION BELT ELECTRONS AND PHENOMENA THAT MEDIATES IT

Contract/Grant #: FA9550-08-1-0140

Reporting Period: 15 March 2008 to 30 November 2010

Achievements

1)We have computed scattering rates due to ULF waves, day-side and night-side chorus waves, EMIC waves, hiss waves in the regions of plumes and inside the plasmasphere, lightning-generated whistlers, and whistlers produced by VLF transmitters. The computed diffusion coefficients were incorporated into our 3D Versatile Electron Radiation Belts (VERB) diffusion code [Subbotin and Shprits, 2009; Shprits et al,. 2009].

2)We have also showed that another scattering mechanism (bounce resonance scattering) driven by magnetosonic waves plays a very important role for scattering radiation belt electrons [Shprits, 2009]. This scattering mechanism was originally proposed by Roberts and Schulz [1968] for fast Alfve´n waves and has not been studied since then.

3) Our VERB code successfully reproduced the behavior of the radiation belts during the Halloween solar storms in 2003. We have also showed that during extremely strong storms, which have occurred in the past and may occur in the future, relativistic electrons

will populate the inner belt (below 1.5 R_E) , where enhanced relativistic electron fluxes may persist for several years [Shprits et al, 2010].

4) We have developed an analytical technique to map an appropriately power-weighted distribution of chorus waves, from its origin outside the plasmasphere, to fill the volume of the inner magnetosphere. The wave power inside the plasmasphere precisely matches the observed characteristics of the plasmaspheric hiss in L-, frequency distribution, and wave-normal behavior.

5)We have simulated the dynamics of the slot region including scattering by hiss waves, lightning-generated whistlers, scattering by anthropogenic whistlers , and scattering due to Coulomb scattering.

6) We have showed that plasmaspheric hiss waves play an important role in determining the dynamics of the slot region. Lightning-generated whistlers also play an important role by scattering high pitch-angle electrons while the contribution of anthropogenic whistlers is less significant.

Archival publications (published) during reporting period:

1. Y. Y.Shprits (2009), Potential waves for pitch-angle scattering of near-equatorially mirroring energetic electrons due to the violation of the second adiabatic invariant, Geophys. Res. Lett., 36, L12106, doi:10.1029/2009GL038322.
2. Y. Y. Shprits, D. Subbotin, and B. Ni (2009), Evolution of electron fluxes in the outer radiation belt computed with the VERB code, J. Geophys. Res.,114, A11209, doi:10.1029/2008JA013784.
3. D. A. Subbotin and Y. Y. Shprits (2009), Three-dimensional modeling of the radiation belts using the Versatile Electron Radiation Belt (VERB) code, Space Weather, 7, S10001, doi:10.1029/2008SW000452.

4. Shprits et al. (2010) Catastrophic Intensification of the Inner Radiation Belt During Solar Superstorms submitted to Journal of Geophysical Research. .

Papers in preparation:

1) Kim, K.-C., Y. Shprits, D. Subbotin, B. Ni (2010), Understanding the Dynamic Evolution of the Relativistic Electron Slot Region based on a Comparison of 1D and 2D Diffusion Simulations in preparation for Journal of Geophysical Research
2) 1. Bortnik, J., L. Chen, W. Li, and R. M. Thorne, Modeling the evolution of chorus waves into plasmaspheric hiss 1. Ray tracing, to be submitted to the Journal of Geophysical Research
3) Bortnik, J., L. Chen, W. Li, and R. M. Thorne, Modeling the evolution of chorus waves into plasmaspheric hiss 2. Wave distribution, to be submitted to Space Weather

Most significant presentations:

Invited presentations:

1. Subbotin, D. A., Y. Y. Shprits, "Simulation of Radiation belt dynamics with UCLA VERB code", JHU, APL, MD, USA, January 2010.
2. Shprits, Y. Y., "Origin of killer electrons in the Earth radiation belts", ENS, Paris, France, May 2010.
3. Shprits, Y. Y., "Losses and Sources of Relativistic Electrons in the Earth Radiation Belts", UNIVERSAT/LRT workshop, Moscow, Russia, June 2010.
4. Subbotin, D. A., Y. Y. Shprits, "Versatile Electron Radiation Belt (VERB) code", GEM Summer Workshop, Snowmass, CO, June 2010.
5. Shprits, Y.Y., "Combining models and observations to understand the dynamical evolution of the radiation belts", 38th COSPAR Scientific Assembly, Bremen, Germany, July 2010.
6. Shprits, Y.Y., "Profound Intensifications of the Earth Radiation Belts", La Trobe University, Melbourne, VIC, Australia, 2010.

7. Shprits, Y.Y., "Dramatic Intensification of the near-Earth Radiation Environment During Solar Superstorms", IGPP, UCLA, Los Angeles, December 2010
8. Shprits, Y.Y., "How does the seed population make a difference?", ISSI meeting, The Earth's Radiation Belts: Physical Processes and Dynamic Modeling, Bern, Switzerland, 8-11 Feb 2011.
9. Shprits, Y.Y., D.A. Subbotin, K. C. Kim, B. Ni, "Versatile Electron Radiation Belt Code", ISSI meeting, The Earth's Radiation Belts: Physical Processes and Dynamic Modeling, Bern, Switzerland, 8-11 Feb 2011.

Presentations at international meetings:

1. Shprits, Y.Y., and M. Schulz, "Bounce Resonance Scattering of Nearly-equatorially Mirroring Relativistic Electrons", presentation at the Geospace Environment Modeling Workshop, Snowmass, CO, June 2009.
2. K. C. Kim, Y. Y. Shprits, D. A. Subbotin, W. Li, "Two-dimensional VERB radiation belt simulations using geomagnetic activity dependent parameterizations of dayside and nightside whistler-mode chorus", GEM Summer Workshop, Snowmass, CO, June 2010
3. Shprits , Y., D. Subbotin, B. Ni, M. Daae, D. A. Kondrashov, M. Hartinger, K. Kim, K. Orlova, T. Nagai, R. H. Friedel, Y. Chen , "Comparison of the 3D VERB Code Simulations of the Dynamic Evolution of the Outer and Inner Radiation Belts With the Reanalysis Obtained from Observations on Multiple Spacecraft", Fall AGU, San Francisco, CA, December 2010.

   Kim, K., Y. Shprits, D. Subbotin, B. Ni, "Understanding of the Dynamic Evolution of the Relativistic Electron Slot Region due to Radial and Pitch Angle Diffusion", Fall AGU, San Francisco, CA, December 2010.

4. Bortnik, J., R. M. Thorne, N. P. Meredith, and L. Chen, "Numerical modeling of plasmaspheric hiss characteristics", American Geophysical Union, Fall Meeting 2009, abstract #SM44A-07.

1. Bounce resonance

We have computed scattering rates due to ULF waves, day-side and night-side chorus waves, EMIC waves, hiss waves in the regions of plumes and inside the plasmasphere, lightning-generated whistlers, and whistlers produced by VLF transmitters.

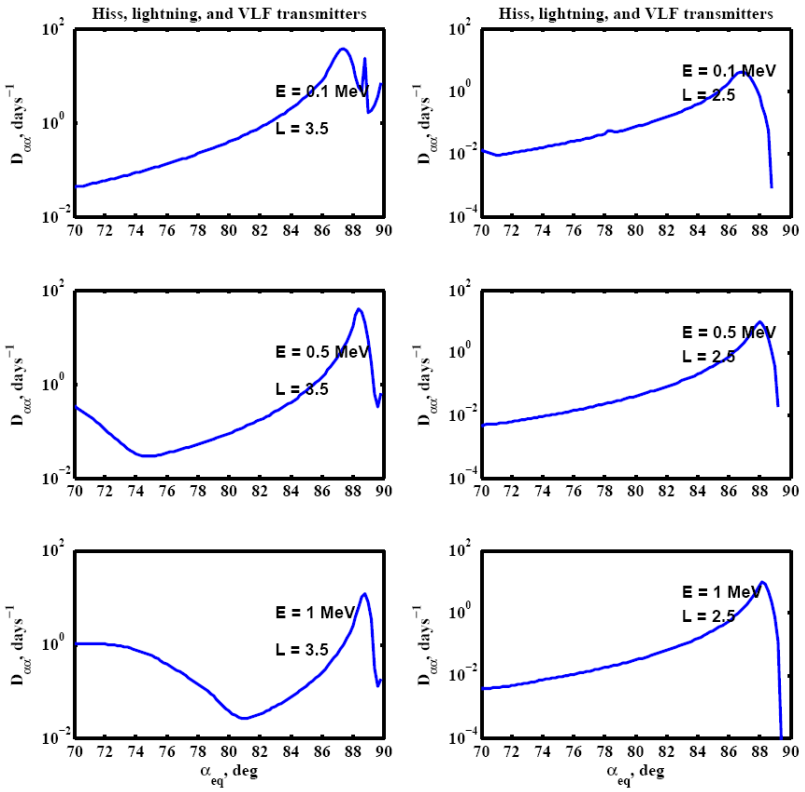

Figure 1. Bounce and drift averaged pitch-angle diffusion coefficients for scattering electrons at 0.1, 0.5 and 1 MeV, due to resonant scattering by plasmaspheric hiss, lightning-generated whistlers, and VLF transmitters.

We have also showed that another scattering mechanism (bounce resonance scattering) driven by magnetosonic waves plays a very important role for scattering radiation belt

electrons [Shprits, 2009]. This scattering mechanism was originally proposed by Roberts and Schulz [1968] for fast Alfve´n waves and has not been studied since then.

Figure 1 (left row) shows that pitch-angle scattering outside of the slot region, at L=3.5, can provide rather weak but still non-zero scattering of electrons up to 90° pitch-angle. In the slot region at L=2.5, the combination of whistler-mode waves cannot affect electrons above ~88-89° for all considered energies of 100 keV, 500 keV and 1 MeV.

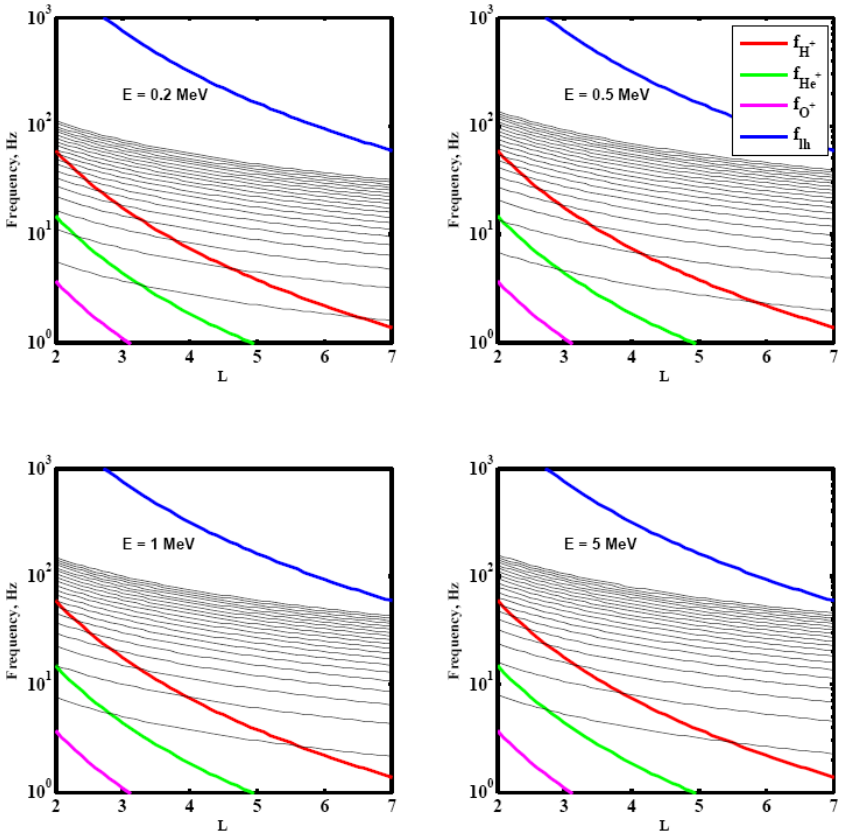

Figure 2. Harmonics of the bounce resonance frequencies as a function of L-shell. Colored bold lines show Hydrogen, Helium, and Oxygen gyro frequencies.

Figure 2 shows the first to the twentieth harmonics of the bounce frequency as a function of L-shell computed for the dipole field. The bold red line shows hydrogen

gyrofrequency, computed for the dipole magnetic field. The bold blue line shows the lower hybrid frequency. For a broad range of energies from 200 keV to 5 MeV and a broad range of L-shells, multiples of the bounce frequency lie between the hydrogen gyro-frequency and the lower-hybrid frequency where magnetosonic waves are observed. The absence of scattering rates for equatorially mirroring electrons indicates that another scattering process affecting electrons mirroring very closely to the geomagnetic equator is required to explain the global coherency of electron fluxes. In this study, we showed that magnetosonic waves and EMIC waves can violate the second adiabatic invariant of nearly equatorially mirroring electrons and plausibly provide pitch-angle scattering for a wide range of electron energies and L-shells inside and outside the plasmasphere. Violation of the second adiabatic invariant will also result in the random change of parallel energy, which may also provide an in-situ acceleration of electrons by means of local energy diffusion.

2. VERB code simulations of the Halloween storm

The computed diffusion coefficients were incorporated into our 3D Versatile Electron Radiation Belts (VERB) diffusion code [Subbotin and Shprits, 2009; Shprits et al,. 2009].

VERB diffusion code can reproduce and explain the dynamical evolution of the electron radiation belts during one of the most unusual episodes of geomagnetic activity ever observed in space (Figure 3). Since in its current formulation the VERB code does not use measurements for any of the boundary conditions or initial conditions and is driven only by the geomagnetic index Kp, the VERB code can predict the possible consequences of an even stronger geomagnetic storm that may occur in the future or veoccurred in the past.

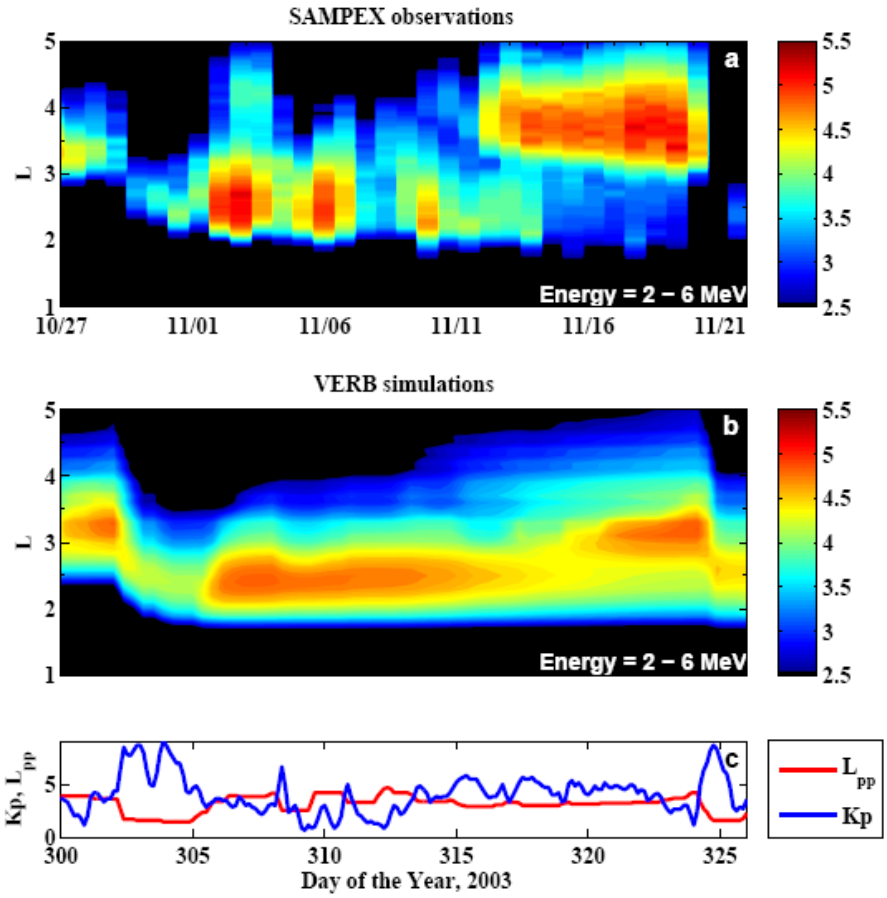

Figure 3. (a) SAMPEX observations of 2 - 6 MeV electron fluxes in ($\log_{10}$(cm^{-2} sr^{-1} sec^{-1})) during the 2003 Halloween storms, DOY 300 - 326 (October 27 - November 22) 1/2 day averaged. Fluxes are presented as a function of time and distance from the Earth in R_E (Earth radii). Averaging is applied to eliminate periodic variations associated with the spacecraft passing over the regions with weak magnetic fields, usually referred to as the South Atlantic Anomaly. (b) VERB code simulations of the dynamics of the radiation belts' 2- 6 MeV electron omni-directional fluxes modeled at the altitude of 850 km in a dipole field in ($\log_{10}$(cm^{-2} sr^{-1} sec^{-1})). A one-day moving average is applied. Unlike in the radial diffusion studies that used data at the outer radial boundary, the VERB code used for this study does not utilize observations and is driven by the Kp index only. The outer

boundary condition is set up at L = 7 and its variation is parameterized by the Kp index. (c) Evolution of the Kp index used for parameterizations of waves and modeled plasmapause location Lpp (*24*).

Our observations of the radiation belts in space are limited to only 3-4 solar cycles. Coronal mass ejections (CME) on the Sun may produce even stronger storms than those observed in space over the last 3-4 decades. While the in-situ observational data set is a very short indirect measurement of the intensity of a storm, taken from ground measurements or visual measurements date back to the 17^{th} century. While ground disturbance during a regular storm is on the scale of -50 to -100 nT, during the recent Halloween super storms, when the slot regain between the two belts was populated, the disturbances on the ground were on the scale of -400nT.

Possibly the strongest ever observed geomagnetic storm occurred on Spetember, 1859. It was also the first ever visually observed storms. This "perfect storm" is usually called the 'Carrington' storm, after one of the first witnesses to observe and document this storm [Carrington, 1895]. Using measurements of the magnetic field component from the Clabea Observatory in Bombay/Mumbai taken during 1846-1867, Tsurutani et al. [2003] inferred that disturbances on the ground produced by such a storm may have exceeded 1600 nT, which is approximately four times as large as was observed during the recent Halloween storms. Other strong storms, which were likely weaker than the 'Carringtorn' storm, occurred in 1890, 1909, 1946, 1956 and 1960, all before extensive in-situ observations were available [Shea, 2006].

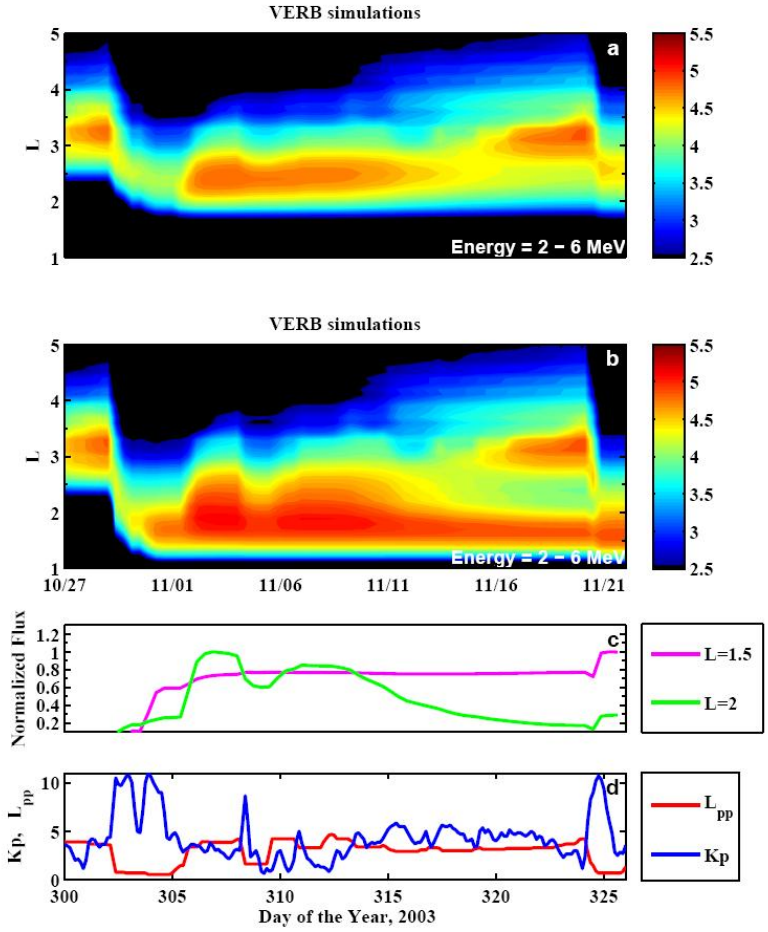

Figure 4. (a) VERB code simulations of the dynamics of the radiation belts' 2 - 6 MeV electron omni-directional fluxes at an altitude of 850 km in ($\log_{10}$(cm^{-2} sr^{-1} sec^{-1})) for the 2003 Halloween storm. (b) same as (a) but during a superstorm with Kp used for parameterizations increased by 2 at all times when the Kp index is greater than 7. (c) Evolution of 2 – 6 MeV radiation belt electron fluxes at an altitude of 850 km for L = 1.5 and L = 2 normalized to the maximum value of the fluxes for a modeled perfect storm. (d) Evolution of the driver of the simulations derived from the Kp index and modeled plasmapause location Lpp. The original time series of Kp index used for the simulations described in section 2 was increased by two when Kp index exceeded 7.

Figure 4A shows the original simulations (same as Figure 3B) presented here for comparison. Figure 4B shows the results of the simulations of a hypothetical, stronger than Halloween storm and compares them to the original simulations (Figure 4A) described in detail in the previous section. While the main phase drop out of fluxes in the simulated 'perfect storm' are stronger then for the simulated Halloween storm, electrons can still penetrate to lower L-shells, deep into the inner radiation zone. Severe erosion of the plasmasphere would allow ULF waves, which may be otherwise reflected at the plasmapause, to penetrate to such low L-shells. These electrons are further accelerated by the local acceleration and result in stronger 2-6 MeV fluxes and a larger special extent of fluxes. The modeled storm on November 20 also diffused electrons to such low L-values and further increased fluxes below L=1.5

The main difference between the evolutions of fluxes is that while at the outer edge of the inner zone fluxes decay on the time-scale of 5-10 days, fluxes in the heart of the inner zone remain practically unchanged during the simulation of the October 29th storm. A modeled consequence of a new flare on day 324 further increases fluxes at L=1.5.

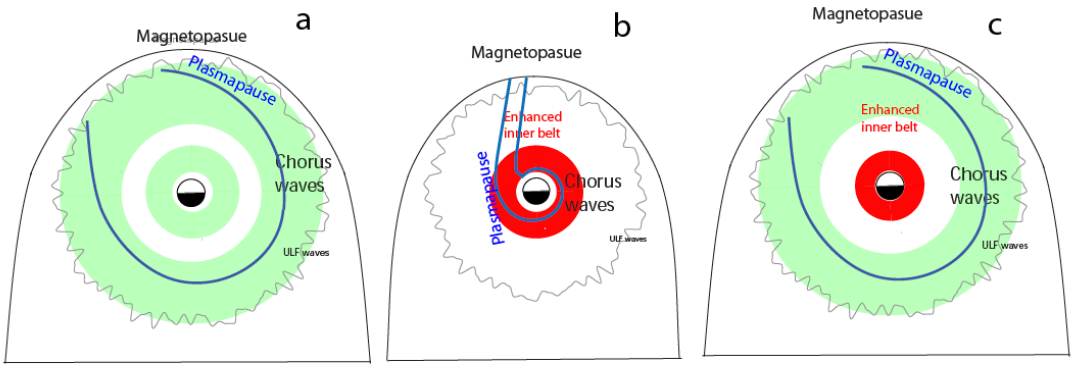

Figure 5. Illustration of the evolution in the Earth's radiation belt fluxes due to a superstorm that compresses the plasmapause to 1.5 Earth radii. Color indicates the intensity of the radiation belt fluxes. (a) Typical two-zone structure of the Earth's radiation belts (b) acceleration of particles during the superstorm, intensification of the inner belt and depletion of the outer belt, and (c) increased inner belt fluxes after the superstorm that may persist for several years. The green color indicates the average amplitude of the radiation belt fluxes. The blue line shows the plasmapause, which is usually outside the slot region and assures that local acceleration may only increase fluxes in the outer radiation belt. During the Halloween storms the plasmapause was compressed to only 2 Earth radii, which did not allow electrons to penetrate into the safe zone below 1.5 Earth radii.

Fig. 5 illustrates the general structure of the radiation belts before (a), during (b), and after (c) such storms. During a superstorm as described above, the plasmapause is eroded and compressed below 1.5 Earth radii, which allows ULF waves to penetrate into the inner belt and diffuse electrons radially much closer to the Earth. Local acceleration in the inner belt, where the magnetic field is strong and the plasma density is low,

enhances inner radiation belt fluxes and will make them several orders of magnitude larger than the outer radiation belt fluxes, depicted as a red belt in Fig. 3 (b) and (c).

These results are consistent with early observations of the electron fluxes after the Starfish nuclear detonation, which populated an artificial radiation belt at L~1.3 as observed by Injun 1 [O'Brien et al., 1962]. Observations of Paulikas et al. [1967] yield lifetimes of ~ 265 days at L=1.3 for electrons above 4.5 MeV. Such a super storm may significantly decrease the lifetime of the polar-orbiting and low-orbiting satellites which traverse the Earth's inner radiation belts.

3 Simulations of the Slot Region Dynamics

In this section, we present simulations of the dynamics of the slot region and compare them with observations.

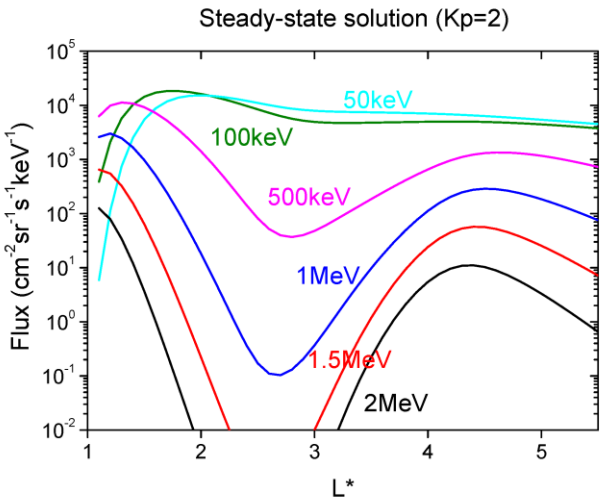

Figure 6. Initial radial profiles of fluxes for various energies obtained from a solution of the steady state radial diffusion equation.

For the initial condition, we used a steady-state solution of the radial diffusion with *Kp*=1 by considering both [I think this is being redundant]components of the radial

diffusion coefficients with the simplified lifetimes described in section 2.1, which is displayed in Figure 6 for various energies as a function of L^*. In Figure 6, one can see the tendency that for a higher energy the slot region is more pronounced and is located more inwardly as already mentioned. Based on the initial flux profiles, we have also solved both the 1-D and 2-D diffusion equations and compared them to each other.

Based on the assumptions above and by solving the Fokker-Planck equation for the radiation belts, we have conducted a 2D diffusion simulation of the time evolution of the 1MeV electron flux for an equatorial pitch angle $\alpha_0 \sim 90^o$. The result is displayed in Figure 7c. For comparison, we also present the corresponding CRRES observations (Figure 7a) and a 1-D radial diffusion simulation (Figure 7b). In Figure 7c, one can see that our diffusion model predicts the instantaneous location of the upper boundary of the slot region, a slot region, and stable inner belts, which shows a general good agreement with the CRRES observations.

Now we model more realistic situations by taking into account several factors: (1) the motion of the plasmapause in response to the *Kp* variation (2) the flux variation at the outer boundary (L^*=5.5) as shown in Figure 5 (middle) and (3) pitch-angle scattering by day-night chorus waves outside the plasmapause for which the bounce-averaged pitch angle diffusion coefficients are calculated. The readers are referred to the work by *Shprits et al.* [2009] for more detailed descriptions of the chorus model. For comparison, we have also conducted a 1-D radial diffusion simulation with the empirical lifetimes taken from *Shprits et al.* [2006].

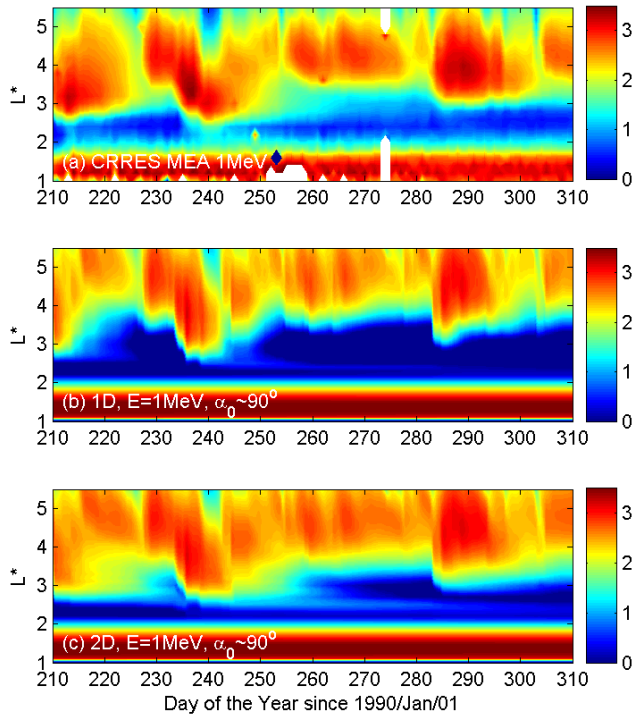

Figure 7. Time evolution of 1MeV electron fluxes with equatorial pitch angle of α_0~90° based on **(a)** CRRES MEV 1MeV observations **(b) a** 1-D and **(c)a** 2-D diffusion simulation with a variable outer boundary.

References

Agostinelli S. et al., Geant4 - A Simulation Toolkit, Nuclear Instruments and Methods **A** 506 250-303 (2003)

Baker, D. N. How to cope with Space Weather, *Science* **297**(5586), 1486-1487(2002).

Baker, D. N., Kanekal, S. G., Li, X., Monk, S. P., Goldstein, J. & Burch, J. L. An extreme distortion of the Van Allen belt arising from the 'Hallowe'en' solar storm in 2003, *Nature* **432**, 878-881, doi:10.1038/nature03116 (2004).

Carpenter, D. L. & Anderson, R. R. An ISEE/whistler model electron density in the magnetosphere, *J. Geophys. Res.* **97**, 1097–1108 (1992).

Carrington, R. C. Description of a singular appearance seen in the Sun on Speterber 1, 1859, *Mon. Not. R. Astron. Soc.*, XX, 13 (1859).

Eddy, J. A. The Maunder Minimum, *Science* **192** (4245), 1189-1201(1976).

Friedel, R. H. W., Reeves, G. D. & Obara, T. Relativistic electron dynamics in the inner magnetosphere – a review, *J. Atmos. Sol. Terr. Phys.* **64,** 265–282 (2002).

Hartinger, M., Moldwin, M. B., Angelopoulos, V. Takahashi, K., Singer, H. J., Anderson, R. R., Nishimura, Y. & Wygant, J. R. Pc5 wave power in the quiet-time plasmasphere and trough: CRRES observations, *Geophys. Res. Lett.* **37**, L07107, doi:10.1029/2010GL042475 (2010).

Hess, W. N., Mead, G. D. & Nakada, M. P. Advances in particles and field research in the satellite era, *Rev. Geophys.* **3**(4), 521-570 (1965).

Horne, R. B. & Thorne, R. M. Potential wave modes for electron scattering and stochastic acceleration to relativistic energies during magnetic storms, *Geophys. Res. Lett.* **25**, 3011 (1998).

Horne, R. B., Thorne, R. M., Shprits, Y. Y., Meredith, N. P., Glauert, S. A., Smith, A. J., Kanekal, S. G., Baker, D. N., Engebretson, M. J., Posch, J. L., Spasojevic, M., Inan, U. S., Pickett, J. S. & Decreau, P. M. E. Wave acceleration of electrons in the Van Allen radiation belts, *Nature* **437**(7056), 227-230, doi:10.1038/nature03939 (2005b).

Hudson, M. K., Elkington, S. R., Lyon, J. G., Goodrich, C. C. & Rosenberg, T. J. Simulation of radiation belt dynamics driven by solar wind variation, in *Sun-Earth Plasma Connections* (eds Burch, J. L., Carovillano, R. L. & Antiochos, S.

K.) *Geophysical Monograph Series* Vol. 109 171-182 (American Geophysical Union, Washington DC, 1999).

Lanzerotti, L. J. Space Weather Effect on Technologies, in *Space Weather* (eds Song, P., Singer, H. J. & Siscoe, G. L.) *Geophysical Monorgaph Series* Vol. 125 11-22 (American Geophysical Union, Washington, DC, 2001).

Lyons, L. R. & Thorne, R. M. Equilibrium structure of radiation belt electrons, *J. Geophys. Res.* **78**, 2142 (1973).

Meredith, N. P., R. B. Horne, R. H. A. Iles, R. M. Thorne, D. Heynderickx, and R. R. Anderson, Outer zone relativistic electron acceleration associated with substorm-enhanced whistler mode chorus, *J. Geophys. Res., 107*(A7), 1144,10.1029/2001JA900146 (2002).

Millan, R. M. & Thorne, R. M. Review of radiation belt relativistic electron losses, *J. Atmos. Sol. Terr. Phys.* **69**, 362 (2006).

Miyoshi, Y., Morioka, A., Obara, T., Misawa, H., Nagai, T. & Kasahara, Y. Rebuilding process of the outer radiation belt during the 3 November 1993 magnetic storm: NOAA and Exos-D observations, *J. Geophys. Res.* **108**(A1), 1004, doi:10.1029/2001JA007542 (2003).

Odenwald, S., Green, J. & Taylor, W. Forecasting the impact of an 1859-calible superstorm on satellite resources, *Advances in Space Research, **38,*** 280-297, (2006).

Otani, S., Miyoshi, Y., Singer, H. J. & Weygand, J. M. On the loss of relativistic electrons at geosynchronous altitude: Its dependence on magnetic configurations

and external conditions, *J. Geophys. Res.* **114**, A01202, doi:10.1029/2008JA013391 (2009).

Paulikas, G. A., Blake, J. B. & Freden, S. C. Inner-zone electrons in 1964 and 1965, *J. Geophys. Res.* **72**(7), 2011-2020 (1967).

Schulz, M. & Lanzerotti, L. J. *Particle Diffusion in the Radiation Belts* (Springer, New York, 1974).

Shea, M. A. The Great Historical Geomagnetic Storm of 1859: A Modern Look, *Adv. Space Res.* **38**(2), 115, doi:10.1016/j.asr.2006.09.002 (2006).

Shprits, Y. Y., Elkington, S. R., Meredith, N. P. & Subbotin, D. A. Review of modeling of losses and sources of relativistic electrons in the outer radiation belts: I. Radial transport, *J. Atmos. Sol. Terr. Phys.* **70**, 1679-1693, doi:10.1016/j.jastp.2008.06.008 (2008a).

Shprits, Y. Y., Li, W. & Thorne, R. M. Controlling effect of the pitch angle scattering rates near the edge of the loss cone on electron lifetimes, *J. Geophys. Res.* **111**, A12206, doi:10.1029/2006JA011758 (2006).

Shprits, Y. Y., Subbotin, D. A., Meredith, N. P. & Elkington, S. R. Review of modeling of losses and sources of relativistic electrons in the outer radiation belts: II. Local acceleration and loss, *J. Atmos. Sol. Terr. Phys.* **70**, 1694-1713, doi:10.1016/j.jastp.2008.06.014 (2008b).

Shprits, Y. Y., Thorne, R. M., Friedel, R., Reeves, G. D., Fennell, J., Baker, D. N. & Kanekal, S. G. Outward radial diffusion driven by losses at magnetopause, *J. Geophys. Res.* **111**, A11214, doi:10.1029/2006JA011657 (2006b).

Shprits, Y. Y., Thorne, R. M., Horne, R. B., Glauert, S. A., Cartwright, M., Russell, C. T., Baker, D. N. & Kanekal, S. G. Acceleration mechanism responsible for the formation of the new radiation belt during the 2003 Halloween solar storm, *Geophys. Res. Lett.* **33**, L05104, doi:10.1029/2005GL024256 (2006a).

Spasojevíc, M. & Inan, U. S. Ground based VLF observations near L = 2.5 during the Halloween 2003 storm, *Geophys. Res. Lett.* **32**, L21103, doi:10.1029/2005GL024377 (2005).

Tsurutani, B. T., Gonzalez, W. D., Lakhina, G. S. & Alex, S. The extreme magnetic storm of 1–2 September 1859, *J. Geophys. Res.* **108**(A7), 1268, doi:10.1029/2002JA009504 (2003).